Inorg. Chem. **2008**, *47*, 5355−5359

Efficient Hydrogen Sorption in 8-Connected MOFs Based on Trinuclear Pinwheel Motifs

Hyungphil Chun,*,† Heejin Jung,† Gumae Koo,† Heondo Jeong,‡ and Dong-Kook Kim‡

Department of Applied Chemistry, College of Science and Technology, Hanyang University, 1271, Sa-3 dong, Ansan 426-791, Republic of Korea, and Advanced Process Research Center, Korea Institute of Energy Research, 71-2 Jang-dong, Yuseong-gu, Daejeon 305-343, Republic of Korea

Received February 12, 2008

Two new metal-organic frameworks based on trinuclear pinwheel motifs are prepared using dicarboxylate and diamine ligands. The structure of $[Co_3(bdc)_3(dabco)]$ (**1**) (bdc = 1,4-benzenedicarboxylate; dabco = 1,4-diazabicyclo[2.2.2]octane) is described as pillared layers, whereas $[Co_3(ndc)_3(dabco)]$ (**2**) (ndc = 2,6-naphthalene-dicarboxylate) forms a variation of primitive cubic net with 3D connected pores. The two 8-connected MOFs are thermally stable at 160 and 250 °C for **1** and **2** respectively in the air and possess corrugated channels owing to the high connectivities of the secondary building unit. As a result, they show highly efficient hydrogen sorption capabilities. Especially, a high hydrogen uptake (2.45 wt % at 77 K and 1 bar) is observed for **2** that has the unique combination of high surface area and small portals.

Introduction

Efforts have been made to understand and improve the physisorption of molecular hydrogen in porous materials, especially in metal-organic frameworks (MOFs).[1] Despite the low storage capacities of currently known MOFs within practical temperature ranges, the tunable nature of these modular porous solids is widely believed to hold the keys for future developments.[2] The developments may lead to a safer and more cost-effective option not only for mobile on-board storage[3] but also for large-scale on-site storage systems.

Approaches taken in this direction are either chemical or physical modifications of pore environments, such as metal doping or ion-exchange, toward stronger H_2-sorbent interactions.[4] More obvious strategies, such as replacing transition-metal ions with lighter elements or using organic ligands with an extended backbone,[5] have also been adopted in the hopes of obtaining MOFs with a low density and high surface area, which will be advantageous for gas uptake in weight percentage.

Meanwhile, a proposal has been made to correlate the portal size and pore profiles with the storage capacities of MOFs.[6] The suggestion was based on the observation that MOFs with straight channels and large openings tend to show a relatively low surface coverage by hydrogen molecules.

* To whom correspondence should be addressed. E-mail: hchun@hanyang.ac.kr.

† Hanyang University.

‡ Korea Institute of Energy Research.

(1) (a) Furukawa, H.; Miller, M. A.; Yaghi, O. M. *J. Mater. Chem.* **2007**, *17*, 3197–3204. (b) Park, H.; Britten, J. F.; Mueller, U.; Lee, J.; Li, J.; Parise, J. B. *Chem. Mater.* **2007**, *19*, 1302–1308. (c) Wu, H.; Zhou, W.; Yildirim, T. *J. Am. Chem. Soc.* **2007**, *129*, 5314–5315. (d) Jia, J.; Lin, X.; Wilson, C.; Blake, A. J.; Champness, N. R.; Hubberstey, P.; Walker, G.; Cussen, E. J.; Schröder, M. *Chem. Commun.* **2007**, *840*, 842. (e) Xiao, B.; Wheatley, P. S.; Zhao, X.; Fletcher, A. J.; Fox, S.; Rossi, A. G.; Megson, I. L.; Bordiga, S.; Regli, L.; Thomas, K. M.; Morris, R. E. *J. Am. Chem. Soc.* **2007**, *129*, 1203–1209.

(2) (a) Collins, D. J.; Zhou, H.-C. *J. Mater. Chem.* **2007**, *17*, 3154–3160. (b) Lin, X.; Jia, J.; Hubberstey, P.; Schröder, M.; Champness, N. R. *Cryst. Eng. Comm.* **2007**, *9*, 438–448. (c) Mueller, U.; Schubert, M.; Teich, F.; Puetter, H.; Schierle-Arndt, K.; Pastré, J. *J. Mater. Chem.* **2006**, *16*, 626–636. (d) Rowsell, J. L. C.; Yaghi, O. M. *Angew. Chem., Int. Ed.* **2005**, *44*, 4670–4679.

(3) (a) von Helmolt, R.; Eberle, U. *J. Power Sources* **2007**, *165*, 833–843. (b) Züttel, A. *Mater. Today* **2003**, *6* (9), 24–33.

(4) (a) Dincã, M.; Long, J. R. *J. Am. Chem. Soc.* **2007**, *129*, 11172–11176. (b) Mulfort, K. L.; Hupp, J. T. *J. Am. Chem. Soc.* **2007**, *129*, 9604–9605. (c) Han, S. S.; Goddard III, W. A. *J. Am. Chem. Soc.* **2007**, *129*, 8422–8423. (d) Dincã, M.; Han, W. S.; Liu, Y.; Dailly, A.; Brown, C. M.; Long, J. R. *Angew. Chem., Int. Ed.* **2007**, *46*, 1419–1422.

(5) (a) Han, S. S.; Deng, W.-Q.; Goddard, W. A., III *Angew. Chem., Int. Ed.* **2007**, *46*, 6289–6292. (b) Ma, S.; Sun, D.; Ambrogio, M.; Fillinger, J. A.; Parkin, S.; Zhou, H.-C. *J. Am. Chem. Soc.* **2007**, *129*, 1858–1859. (c) Fang, Q.-R.; Zhu, G.-S.; Jin, Z.; Ji, Y.-Y.; Ye, J.-W.; Xue, M.; Yang, H.; Wang, Y.; Qiu, S.-L. *Angew. Chem., Int. Ed.* **2007**, *46*, 6638–6642.

(6) Chun, H.; Dybtsev, D. N.; Kim, H.; Kim, K. *Chem.—Eur. J.* **2005**, *11*, 3521–3529.

(7) (a) Davies, R. P.; Less, R. J.; Lickiss, P. D.; White, A. J. P. *Dalton Trans.* **2007**, *2528*, 2535. (b) Senkovska, I.; Kaskel, S. *Eur. J. Inorg. Chem.* **2006**, *4564*, 4569. (c) Dincã, M.; Long, J. R. *J. Am. Chem. Soc.* **2005**, *127*, 9376–9377.

10.1021/ic800274w CCC: $40.75
Published on Web 05/06/2008

We think that this is due to the fast diffusion of desorbed hydrogen, limiting chances of readsorption on to the adsorbent surface. Consequently, we set out to study MOFs in which corrugated channels are interconnected to give a high surface area and yet with small portal sizes.

We reasoned that 3D nets based on trinuclear pinwheel motifs may possess such properties. Having the formula $[M_3(O_2C)_6(sol)_n]$, where sol implies for coordinating solvents and $n = 2 \sim 4$, the secondary building unit (SBU) acts as 6-connecting nodes to form narrow channels with a triangular cross-section. In fact, a number of pinwheel-based MOFs has been reported to date, and they are either distorted α−Po nets[7] or bilayer-type 2D nets.[8] However, not many frameworks are known in which the solvent sites of pinwheels are utilized to render extra connectivities in the framework without an interpenetration.[9] Therefore, we used mixed ligands of dicarboxylate and diamine to synthesize MOFs based on trinuclear pinwheel units. Two new MOFs thus obtained are based on the same type of SBUs, but their network topologies are completely different. Their crystal structures and gas sorption properties are reported here.

Experimental Section

Materials and Methods. All of the reagents and solvents were commercially available and used as received. TGA data for **1** and **2** were obtained on a PerkinElmer Pyris 1 and SCINCO S-1000 instruments, respectively, with a heating rate of 10 °C min^{-1}. The TGA data are shown in Figure S1. The IR spectra were recorded on a Varian FTS 1000 instrument (Figure S2). The X-ray powder diffraction patterns were recorded on a Bruker D8 Advance system equipped with a copper-sealed tube ($\lambda = 1.54178$ Å) at a scan rate of 10 s deg^{-1} (Figure 3). The variable-temperature measurements were carried out in the air, and the sample was heated gradually from room temperature with a holding time of at least 30 min at each temperature.

Synthesis of $[Co_3(bdc)_3(dabco)]$ (1). $Co(NO_3)_2 \cdot 6H_2O$ (0.375 g, 1.29 mmol) and H_2bdc (0.214 g, 1.29 mmol) were dissolved in 10.0 mL of DMF. After adding dabco (0.048 g, 0.43 mmol) and CH_3CN (5 mL), the mixture was stirred for 2 h at room temperature. The greenish-blue precipitate was filtered off after centrifuge, and the purple filtrate was put into a glass tube. The tube was flame-sealed and heated to 100 °C for 36 h. Purple crystals of diamond shape were collected, washed with DMF/CH_3CN mixture (1:1 v/v), and dried under vacuum. The yield was 0.322 g or 76% based on $[Co_3(bdc)_3(dabco)(dmf)_2](CH_3CN)(H_2O)$. EA Calcd: C, 46.26; H, 4.39; N, 7.10. Found: C, 46.18; H, 4.12; N, 7.61%. The as-synthesized crystals were soaked in CH_3CN for 2 days, and evacuated by dynamic vacuum at room temperature for 12 h to give the dehydrated form $[Co_3(bdc)_3(dabco)] \cdot 0.5(H_2O)$. EA Calcd: C, 45.59; H, 3.19; N, 3.54. Found: C, 45.39; H, 3.04; N, 3.57%.

Synthesis of $[Co_3(ndc)_3(dabco)]$ (2). $Co(NO_3)_2 \cdot 6H_2O$ (0.155 g, 0.53 mmol) and H_2ndc (0.116 g, 0.54 mmol) were dissolved in 10.0 mL of DMF. After adding dabco (0.020 g, 0.18 mmol) and *o*-xylene (5 mL), the mixture was stirred for 2 h at room temperature. The greenish-blue precipitate was filtered off after centrifugation, and the purple filtrate was put into a glass vial. The vial was tightly sealed and heated to 110 °C for 36 h. Purple crystals of diamond shape were collected, washed with DMF, and soaked in toluene. The yield was 0.173 g or 66% based on $[Co_3(ndc)_3(dabco)] \cdot 6(C_7H_8)$. Elemental analysis calcd for $[Co_3(ndc)_3(dabco)] \cdot 4(C_7H_8) \cdot (H_2O)$: C, 63.79; H, 4.89; N, 2.13. Found: C, 63.76; H, 5.02; N, 2.68%. The as-synthesized crystals were guest-exchanged with CH_3Cl, and evacuated under dynamic vacuum at room temperature for 12 h to give the dehydrated form $[Co_3(ndc)_3(dabco)] \cdot 2(H_2O)$. EA Calcd: C, 52.14; H, 3.54; N, 2.90. Found: C, 52.50; H, 3.31; N, 3.05%.

X-ray Crystallography. For **1**, single crystals were directly picked up from the mother liquor, attached to a glass fiber, and transferred to a cold stream of liquid nitrogen (−100 °C) for data collections. The full hemisphere data were collected on a Siemens SMART CCD diffractometer with Mo Kα radiation ($\lambda = 0.71073$ Å). After the data integration (*SAINT*) and semiempirical absorption correction based on equivalent reflections (*SADABS*), the structure was solved by direct methods and subsequent difference Fourier techniques (*SHEXLTL*). For **2**, single crystals soaked in toluene were picked up with a cryoloop attached to a goniometer head, and transferred to a cold stream of liquid nitrogen (−173 °C). The data collection was carried out using synchrotron X-ray ($\lambda = 0.80000$ Å) equipped with an ADSC Quantum 210 CCD detector at Pohang Accelerator Laboratory. After the data integration (*HKL2000*) and space group determination (*XPREP*), the structure was solved by direct methods and subsequent difference Fourier techniques (*SHEXLTL*). For **1**, all of the framework atoms except for those of disordered DMF solvent were refined anisotropically. After adding hydrogen atoms to their calculated positions, the diffused electron densities resulting from the residual solvent molecules were removed from the data set using the *SQUEEZE* routine of *PLATON*,[10] and the results were attached to the CIF file. For **2**, all of the non-hydrogen atoms were refined anisotropically, including those of the toluene solvent molecules. Details of the data collection and structure refinements are summarized in Table 1.

Gas Sorption Studies. BET gas sorption isotherms were measured with a custom-made vacuum manifold following a standard volumetric technique at 77 K. The gases used were of extra-pure quality (N50 for nitrogen and N60 for hydrogen). For **1**, a crystalline sample soaked in CH_3CN was evacuated under a dynamic vacuum (10^{-3} Torr) at room temperature for 12 h. For **2**, the sample was guest-exchanged with $CHCl_3$ before activation under a dynamic vacuum at room temperature for 12 h. These activation processes (guest-exchange with low-boiling solvents and evacuation at room temperature) give consistent and reproducible results in the sorption experiments. A part of the N_2 sorption isotherm in the P/P_0 range 0.10−0.30 was fitted to the BET equation to estimate the BET surface area (Figure S3 in the Supporting Information). For the Langmuir surface area, data from the whole adsorption isotherm were used (Figure S4 in the Supporting Information). For **2**, the Langmuir fit was used to extrapolate the sorption data into a high-pressure region, and the result is shown in Figure S5 in the Supporting Information. The high pressure sorption of hydrogen by **2** was measured at 298 K with a locally built equipment using a volumetric technique. The instrumental setup is shown in Figure

(8) (a) Yang, G.-D.; Dai, J.-C.; Lian, T.-X.; Wu, W.-S.; Lin, J.-M.; Hu, S.-M.; Sheng, T.-L.; Fu, Z.-Y.; Wu, X.-T. *Inorg. Chem.* **2007**, *46*, 7910–7916. (b) Wang, Y.; Bredenkötter, B.; Rieger, B.; Volkmer, D. *Dalton Trans.* **2007**, *689*, 696. (c) Williams, C. A.; Blake, A. J.; Hubberstey, P.; Schröder, M. *Chem. Commun.* **2005**, *5435*, 5437.

(9) (a) Sun, J.; Zhou, Y.; Fang, Q.; Chen, Z.; Weng, L.; Zhu, G.; Qiu, S.; Zhao, D. *Inorg. Chem.* **2006**, *45*, 8677–8684. (b) Wang, X.-L.; Qin, C.; Wang, E.-B.; Su, Z.-M. *Chem.—Eur. J.* **2006**, *12*, 2680–2691. (c) Lee, J. Y.; Pan, L.; Kelly, S. P.; Jagiello, J.; Emge, T. J.; Li, J. *Adv. Mater.* **2005**, *17*, 2703–2706. (d) Pan, L.; Liu, H.; Lei, X.; Huang, X.; Olson, D. H.; Turro, N. J.; Li, J. *Angew. Chem., Int. Ed.* **2003**, *42*, 542–546.

(10) Spek, A. L. *PLATON, A Multipurpose Crystallographic Tool*; Utrecht University: Utrecht, The Netherlands, 2001.

Table 1. Summary of Crystal Data and Structure Refinements for **1** and **2**

	1·2dmf	**2**·4.5$C_6H_5CH_3$
empirical formula	$C_{36}H_{38}N_4O_{14}Co_3$	$C_{73.5}H_{66}N_2O_{12}Co_3$
fw	927.51	1346.07
T (K)	173(2)	100(2)
λ (Å)	0.71073	0.80000
cryst syst (space group)	monoclinic ($C2/c$)	
a (Å)	31.717(3)	20.136(4)
b (Å)	9.4333(9)	21.190(4)
c (Å)	18.1739(18)	17.292(4)
β (°)	119.894(2)	93.78(3)
V (Å^3)	4714.1(8)	7362(3)
Z	4	4
ρ_{calcd} (g/cm^3)	1.307	1.214
μ (mm^{-1})	1.103	0.725
F(000)	1900	2792
cryst size (mm^3)	0.50 × 0.40 × 0.15	0.37 × 0.27 × 0.15
reflns collected	14 131	13 700
independent reflns	5617 (R_{int} = 0.0223)	7485 (R_{int} = 0.0497)
T_{max}/T_{min}	0.8520/0.6085	0.8990/0.7752
data/restraints/params	5617/0/254	7485/42/465
GOF on F^2	1.137	1.101
final R indices [$I > 2\sigma(I)$]	R1 = 0.0460, wR2 = 0.1140	R1 = 0.0761, wR2 = 0.2251
R indices (all data)	R1 = 0.0510, wR2 = 0.1156	R1 = 0.0803, wR2 = 0.2287
extinction coefficient		0.0140(9)
largest diff. peak/hole (e/Å^3)	0.781/−1.017	1.594/−0.850

S6 in the Supporting Information, and the results in Figure S7 in the Supporting Information.

Results and Discussion

Solvothermal reactions of $Co(NO_3)_2 \cdot 6H_2O$, H_2bdc and dabco in a mixed solvent system produce purple-colored single crystals of [Co_3(bdc)$_3$(dabco)(dmf)$_2$] which is desolvated to give the porous net [Co_3(bdc)$_3$(dabco)] (**1**). Similar reactions using H_2ndc in place of H_2bdc give a crystalline material which is characterized to be [Co_3(ndc)$_3$(dabco)] (**2**). It is noted that the dark purple colors of **1** and **2** gradually turn to red when the solids are cooled below 200 K (see Supporting Information). This thermochromic behavior may be an indication for subtle changes in the geometry of Co(II) ions which are coordinatively unsaturated. X-ray diffraction studies on the single crystals of **1** and **2** reveal that both compounds are framework solids based on 8-connecting pinwheel nodes.[11]

In the structure of **1**, the six bdc linkers around one pinwheel unit connect 6 neighboring pinwheels to form 2D bilayers with a triangular pattern, and dabco ligands act as pillars between two such layers (Figure 1a−b). The triangular openings are not large enough for the passage of guest molecules, and thus the guest-accessible void in **1** is found sandwiched between the two layers (Figure 1c−d). That is, the pores of the 3D net of **1** are two-dimensional in nature.

The single crystal structure of **2** was determined using high-flux X-ray from a synchrotron beam line after guest-exchange with toluene. Such measures were necessary because the resolution and overall quality of the structure determined using conventional X-ray on as-synthesized crystals was rather poor. The toluene molecules that fill the void of **2**, 57% of the crystal volume,[10] were clearly located from the difference Fourier maps and fully refined. They are found to form complicated $\pi\cdots\pi$ and CH$\cdots\pi$ contacts among themselves or with the framework atoms.

Understanding the 3D structure of **2** requires a viewpoint that is different from that of **1**. The pinwheel SBU in **2** can be seen as a distorted octahedral node with two extra linkages of dabco ligands (part a of Figure 2). Then, the structure of **2** is simplified to a distorted primitive cubic net with an additional linkage along the body diagonal of each primitive cell (part b of Figure 2). Triangular channels are evident when the structure is viewed along the direction of the N−Co

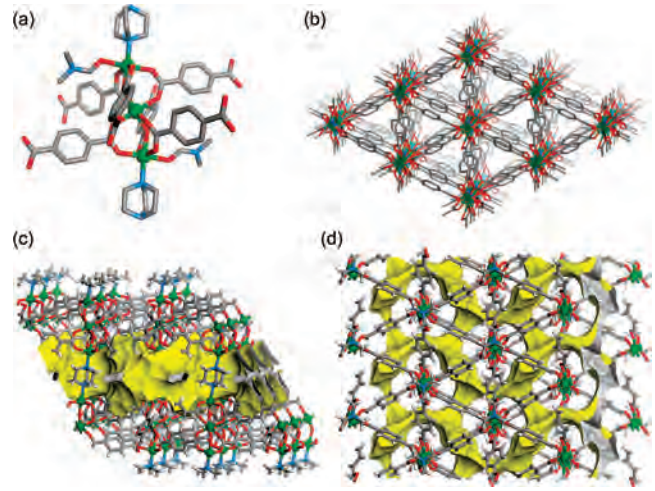

Figure 1. The pinwheel SBU (a) and expanded view along the N−Co bonds (b) of **1**. Hydrogen atoms are omitted. (c−d) Side and top view of the 2D channels depicted in yellow.

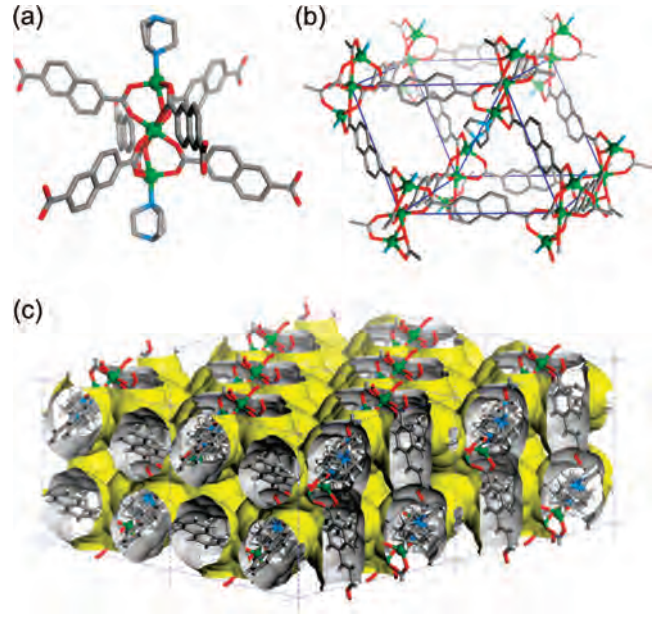

Figure 2. The pinwheel SBU (a) and its role as 8-connecting node in a local view (b) of **2**. (c) Extended view of **2** showing the solvent-accessible void with the inner surface emphasized in yellow. Dashed lines are the unit cell edges.

(11) (a) For 8-connected MOFs based on different building units, see Hill, R. J.; Long, D.-L.; Champness, N. R.; Hubberstey, P.; Schröder, M. *Acc. Chem. Res.* **2005**, *38*, 337–350. (b) Wang, X.-L.; Qin, C.; Wang, E.-B.; Su, Z.-M.; Xu, L.; Batten, S. R. *Chem. Commun.* **2005**, *4789*, 4791. (c) Chun, H.; Kim, D.; Dybtsev, D. N.; Kim, K *Angew. Chem., Int. Ed.* **2004**, *43*, 971–974.

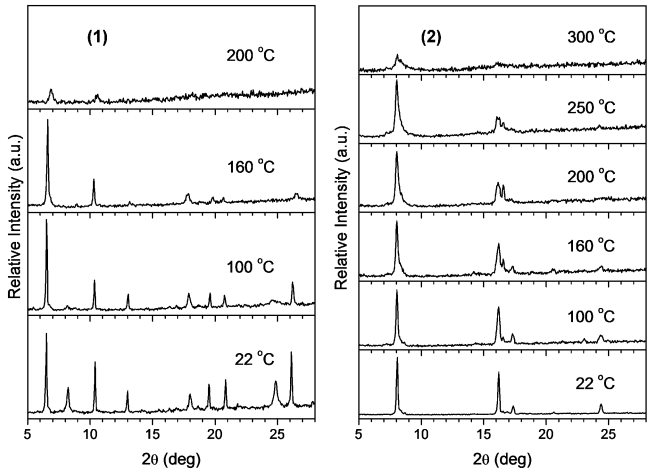

Figure 3. Temperature-dependent XRD patterns of as-synthesized **1** (left) and **2** measured upon gradual heating from room temperature.

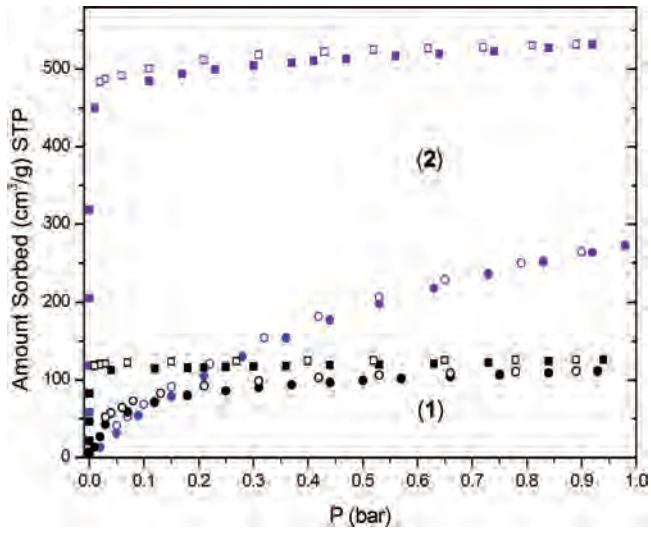

Figure 4. Nitrogen (squares) and hydrogen (circles) sorption isotherms measured at 77 K. Filled and open symbols denote sorption and desorption, respectively.

bonds. Taking the van der Waals surface of the framework into account, the triangular channels of **2** would allow an imaginary sphere with a 4.5 Å diameter pass-through. For **2**, therefore, both the framework and the pores are 3D as shown in part c of Figure 2.

Thermal gravimetric analyses on the as-synthesized forms of **1** and **2** show that the decomposition of the frameworks occurs no earlier than 350 °C (Supporting Information). However, **1** and **2** may have collapsed without being decomposed at temperatures above 200 and 300 °C, respectively, judging from the variable-temperature measurements of X-ray powder diffractions (Figure 3). The relatively low thermal stability for **1** is probably because the net of **1** is more strained than that of **2** due to the shorter dicarboxylate linkers.

The accessibility and utility of the pores of **1** and **2** were examined by gas sorption studies. Both **1** and **2** show reversible type I behavior in the nitrogen gas sorption experiments (Figure 4). The isotherms are typical for microporous MOFs. The BET (Langmuir) surface areas deduced from the isotherms are 360 (538) and 1502 (2293) m^2/g for **1** and **2**, respectively. The total pore volumes of **1** and **2** are 0.195 and 0.822 cm^3/g, respectively.

For hydrogen gas, the maximum uptake by **1** at 77 K and 0.93 bar is moderate at 1.00 wt % and is nearly saturated. However, the relatively small pore volume of **1** leads to the density of 51.2 g/L for hydrogen adsorbed in **1**. This is 72% of the density of liquid hydrogen at 20 K and 1 bar (71.1 g/L),[12] which supports the idea of storing hydrogen gas through physisorption in porous MOFs.

As expected, the sorption of hydrogen in **2** is significantly higher than that in **1** and results in 2.45 wt % uptake at 77 K and 0.98 bar. In fact, this is close to the highest value known in the literature for MOFs under the same condition, which is 2.59 wt %.[13] Meanwhile, the density of hydrogen adsorbed in **2** (29.8 g/L) is much lower than that in **1** because the isotherm is not saturated at 77 K and 1 bar. When the isotherm is extrapolated into a high-pressure region using a Langmuir fit ($R = 0.9998$), the H_2 adsorption by **2** is expected to saturate with approximately 4.2 wt % uptake at 77 K and 40 bar (Supporting Information). In such a circumstance, the density of adsorbed hydrogen would reach 51.1 g/L. We also measured the hydrogen sorption in **2** under high pressures at room temperature (Supporting Information). The uptake that continuously increases with increasing pressure reaches 0.89 wt % at 17.2 bar and 298 K. Taking the total pore volume of **2** determined from N_2 sorption at 77 K (0.822 cm^3/g), this is equivalent to the density of 10.8 g/L for adsorbed hydrogen. For comparison, the hydrogen gas compressed to 100 bar at 300 K has a density of 7.62 g/L.[12] Although these results do not satisfy the standards set for practical applications,[3] at least the potential has been proven that porous MOFs can be an effective storage medium for hydrogen gas within moderately high pressure ranges.

The efficient hydrogen sorption in the title frameworks is believed not because of specific chemical moieties or metal ions but because of the physical characteristics, such as the size and shape of the channels. Especially, **2** is unique in that it offers a high surface area and porosity, but allows only small free openings. A close examination of the solvent-accessible surface shown in part c of Figure 2 reveals that the width of the interconnected channels are in the range of $4 \sim 6$ Å. This feature is uncommon in MOFs having comparable surface areas and may become an important guide for targeted design and synthesis in future works. We expect that increasing the overall porosity while maintaining the size of portals and channels similar to that of **2** may result in even higher storage capacities. Using mixed ligands in 8-connected pinwheel-based nets, as in this work, is advantageous in this context because it allows modifications at either or both of the dicarboxylate or diamine linkers.

In conclusion, we have targeted and successfully synthesized two porous MOFs, which are based on trinuclear pinwheel SBUs and simple organic ligands. The two MOFs

(12) *CRC Handbook of Chemistry and Physics*, 88th Ed.; Lide D. R., Ed.; CRC Press: FL, 2007.
(13) Lin, X.; Jia, J.; Zhao, X.; Thomas, K. M.; Blake, A. J.; Walker, G. S.; Champness, N. R.; Hubberstey, P.; Schröder, M. *Angew. Chem., Int. Ed.* **2006**, *45*, 7358–7364.

possess void structures that withstand a complete evacuation. One of the two 8-connected nets, $[Co_3(ndc)_3(dabco)]$, shows a highly efficient hydrogen sorption due to the unusual combination of high surface area and narrow channels. The tunable nature of the title frameworks, which are composed of two different ligands, implies that the more efficient storage of molecular hydrogen should be possible through physisorption in porous MOFs.

Acknowledgment. This work was supported by the Korea Research Foundation Grant funded by the Korean Government (MOEHRD) (KRF-2006-331-C00157 and KRF-2005-070-C00068). H.C. thanks the Pohang Accelerator Laboratory for a beamline use (2007-2041-14). H.C. is grateful to Prof. K. Kim (POSTECH, Korea) for allowing access to XRPD. H.C. dedicates this article to Prof. Ivan Bernal (University of Houston) on his retirement.

Supporting Information Available: The plots of TGA and IR, diagram for instrumental setup, analysis of gas sorption data, and crystallographic information files (CIF). This material is available free of charge via the Internet at http://pubs.acs.org.

IC800274W